ORGANOMETALLICS

Article

pubs.acs.org/Organometallics

# Reactivity of Bridged and Nonbridged Zirconocenes toward Biorenewable Itaconic Esters and Anhydride

Fernando Vidal and Eugene Y.-X. Chen*

Department of Chemistry, Colorado State University, Fort Collins, Colorado 80523-1872, United States

Supporting Information

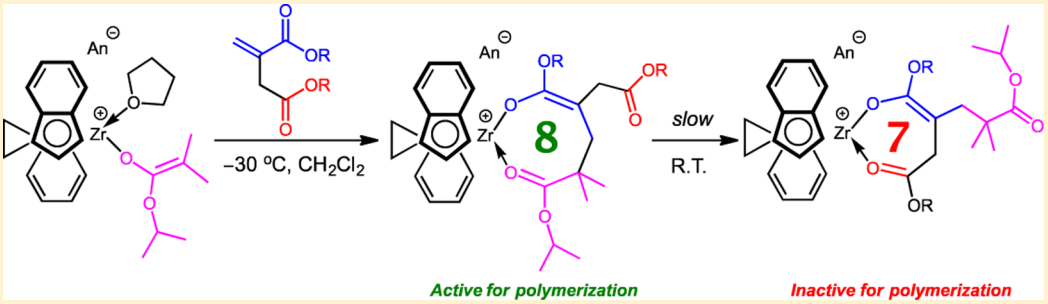


**ABSTRACT:** This work investigates the reactivity of neutral and cationic complexes of both bridged *ansa*-zirconocenes, *rac*-[$C_2H_4$(Ind)$_2$]ZrMe[OC(O$^i$Pr)=CMe$_2$] (**1**) and *rac*-[$C_2H_4$(Ind)$_2$]Zr$^+$(THF)[OC(O$^i$Pr)=CMe$_2$][MeB($C_6F_5$)$_3$]$^-$ (**1**$^+$), and nonbridged zirconocenes, Cp*($^n$PrCp)ZrMe[OC(O$^i$Pr)=CMe$_2$] (**13**) and Cp*($^n$PrCp)Zr(THF)[OC(O$^i$Pr)=CMe$_2$]$^+$[MeB($C_6F_5$)$_3$]$^-$ (**13**$^+$), toward biorenewable itaconic dialkyl esters (itaconates) and anhydride (IA). Behaving *similarly*, both cationic complexes **1**$^+$ and **13**$^+$ react readily with itaconates to form cleanly single monomer addition products, eight-membered-ring metallacycles **2** and **15**, respectively, and neutral enolate complexes **1** and **13** insert 1 equiv of IA to afford single-IA-addition products **5** and **17**. Behaving *differently*, eight-membered-ring chelates **2** derived from the bridged metallocene framework undergo slow isomerization at room temperature via ligand exchange between the coordinated and uncoordinated ester groups to form thermodynamically favored seven-membered-ring chelates **4**, while eight-membered chelates **15** derived from the sterically more crowded unbridged metallocene framework are stable at room temperature and do not undergo such isomerization. The above cationic complexes exhibit no reactivity toward further additions of itaconates. Replacing itaconates with more basic monomers such as *N*,*N*-dimethylacrylamide that can ring open the chelating resting intermediate, however, brings about effective and controlled polymerization by eight-membered Zr-itaconate metallacycles **2** and **15**, but not seven-membered **4**, producing either highly isotactic polymers (>99% *mm*, by **2**) or polymers with narrow molecular weight distributions ($Đ$ < 1.19, by **15**). These results further highlight the *ansa* effects in the metallocene polymerization chemistry and the importance of the formation and ring opening of the eight-membered chelating intermediates involved in the metallocene-mediated conjugate-addition polymerization.

## INTRODUCTION

Biomass-derived itaconic acid has received increased attention in recent years as a more sustainable alternative to petroleum-based building blocks for obtaining new renewable polymeric materials, due to the structural resemblance of its derivatives to other widely used acrylic monomers, such as methyl methacrylate (MMA).[1,2] Its large worldwide production by fermentation with the fungus *Aspergillus terreus* is still by far the largest source of itaconic acid and its derivatives[3−5] and has uplifted this dicarboxylic ene-bearing monomer as one of the most important chemical platforms derived from renewable resources.[6−8] Among other applications, dialkyl ester derivatives of itaconic acid, or itaconates, such as dimethyl itaconate (DMIA) and diisopropyl itaconate (D$^i$PrIA), and cyclic itaconic anhydride (IA) have been explored as vinyl monomers by free radical polymerization with $\alpha,\alpha'$-azobis(isobutyronitrile)[9−12] and atom transfer radical polymerization.[13,14] More recently, efforts have been made to exploit the use of the diacid (or diester) units as the polymerizable handle in condensation polymerization to obtain unsaturated polyesters, and their applications have been expanded to drug delivery, shape memory, and elastomeric materials.[15,16] However, to the best of our knowledge, such monomers have not been examined using the metal-mediated coordination polymerization method, which has the potential to produce stereoregular itaconate polymers for enhanced physical and chemical properties.

Coordination−addition polymerization of conjugated acrylic monomers mediated by cationic chiral *ansa*-zirconocenium ester enolate catalysts has proven to be a powerful method for obtaining highly stereoregular polymers in a living/controlled manner.[17] For instance, highly isotactic poly(methyl methacrylate) (PMMA) with isotacticity [*mm*] triads up to 97% has been readily produced at room temperature by the $C_2$-ligated

**Received:** May 8, 2017
**Published:** July 12, 2017




DOI: 10.1021/acs.organomet.7b00358
*Organometallics* 2017, 36, 2922−2933

zirconocenium ester enolate complex *rac*-(EBI)$Zr^+$(THF)[OC(O$^i$Pr)=$CMe_2$][$MeB(C_6F_5)_3$]$^-$ (**1**$^+$, EBI = ethylenebis(indenyl)) very efficiently, with high to near-quantitative catalyst efficiency.[18,19] Highly syndiotactic PMMA with syndiotacticity [*rr*] triads up to 94% has also been synthesized under ambient conditions, using the $C_s$-ligated zirconocenium ester enolate complex {[$Ph_2C$(Cp)(2,7-$^t$$Bu_2$Flu)]Zr(THF)[OC(O$^i$Pr)=$CMe_2$]}$^+$[$MeB(C_6F_5)_3$]$^-$ (Flu = $\eta^n$-fluorenyl).[20] Other acrylic monomers, such as *N*,*N*-dimethylacrylamide (DMAA), biorenewable butyrolactones such as $\beta$-methyl-$\alpha$-methylene-$\gamma$-butyrolactone, and divinyl monomers such as allyl methacrylate and 4-vinylbenzyl methacrylate were also efficiently polymerized to give highly stereoregular polymers.[21−25] Such polymerizations are typically living or quasi-living, allowing for precise control over the polymer chain structures. The origin of the chemo- and stereoselectivity observed in this precision polymerization of polar vinyl or polar divinyl monomers arises from the enantiomorphic-site-controlled coordination−addition mechanism, in which the fundamental steps of the propagation sequence require the Michael addition of the nucleophilic ester enolate chain end onto the conjugated C=C double bond of the coordinated incoming monomer to form an eight-membered-ring chelate (resting state).[26] In our continued effort to better understand the implications of the resting intermediate in the chain initiation and propagation reactions, we envisioned that the extra ester group in the dialkyl ester itaconates and itaconic anhydride, in comparison to the alkyl group (Me or H) in methacrylates and acrylamides, would present an extra chemical handle to further test the requisites of the chain-growth reaction. Upon addition of the first monomer, the resulting Zr-itaconate metallacycle could exhibit two possible isomers: eight-membered chelate vs seven-membered chelate (Scheme 1).

**Scheme 1. Working Hypothesis on the Possible Single-Monomer-Addition Structures and Their Reactivity toward Subsequent Monomer Additions, Where [Zr]$^+$ Represents Bridged 1$^+$ and Unbridged 13$^+$**

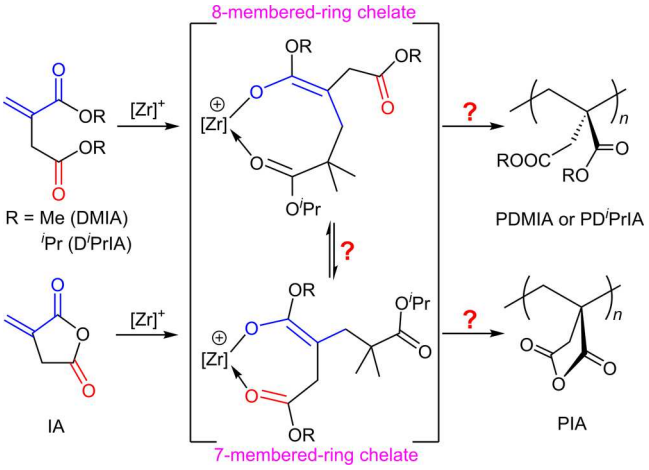


Two important fundamental questions immediately emerge. (1) What are the structure and reactivity of the resulting first-monomer-addition product (eight-membered metallacycle vs seven-membered species)? (2) What are the effects of the metallocene initiator/catalyst structure (bridged vs unbridged) on the resulting addition product? To address these two fundamental questions, we employed two types of metallocenium catalysts in this study: a $C_2$-ligated *bridged ansa*-zirconocenium ester enolate, **1**$^+$, and a sterically encumbered *nonbridged* metallocenium ester enolate, Cp*($^n$PrCp)Zr(THF)[OC(O$^i$Pr)=$CMe_2$]$^+$[$MeB(C_6F_5)_3$]$^-$ (**13**$^+$). Overall, this study has successfully answered the above two fundamental questions and also uncovered not only similar monomer insertion and polymerization chemistry but also some intriguing differences, between these two classes of metallocene complexes.

## RESULTS AND DISCUSSION

**Reactivity of $C_2$-Ligated Bridged *ansa*-Zirconocenium Complexes with Dialkyl Itaconates.** First, we focused our attention on cationic chiral *ansa*-zirconocenium ester enolate **1**$^+$, which is generated in situ from the reaction of *rac*-(EBI)ZrMe[OC(O$^i$Pr)=$CMe_2$] (**1**) with $(C_6F_5)_3$B·THF and is a highly active and efficient metallocene catalyst for the polymerization of a wide variety of polar (meth)acrylic and acrylamide substrates, including the renewable and biomass-derived methylene butyrolactones and other challenging polar divinyl acrylic monomers, with high levels of stereoselectivity and control.[21,25] In sharp contrast, addition of an excess amount of itaconates DMIA, D$^i$PrIA, and IA to **1**$^+$ at ambient or higher temperatures (up to 100 °C) resulted in no monomer conversion even after prolonged periods of time. Thus, we next examined the stoichiometric reactions between catalyst **1**$^+$ and the itaconate monomers to determine whether the origin for this lack of polymerization activity was due to catalyst decomposition or catalytic incompetency for chain initiation and/or propagation.

To this end, we designed a series of NMR-scale stoichiometric reactions to examine the reactivity of the isopropyl ester enolate ligand in **1**$^+$ to undergo the first nucleophilic Michael addition over the conjugated C=C bond of the itaconate monomers, which is a key step for the analogous initiation in the polymerization of (meth)acrylates and acrylamides.[18,19,22,23,27−30] Indeed, the reaction between 1 equiv of DMIA or D$^i$PrIA and the preformed **1**$^+$ at −30 °C in $CD_2Cl_2$ showed instantaneous consumption of the monomers and clean formation of single-addition products **2a**,**b**, respectively (Scheme 2), as bright red solutions. These structures are analogous to those obtained under otherwise identical conditions between **1**$^+$ and MMA (or other acrylamide and divinyl acrylic monomers) and resemble the resting intermediate in the MMA polymerization,[19,23−25,29] except that the newly formed metallocene complexes **2a**,**b** contain an extra noncoordinated carbonyl group derived from the $\beta$-alkyl ester (the nonconjugated ester group) in the itaconates. Thus, detection of **2a**,**b** indicated that the $\alpha$-alkyl ester (the conjugated ester group) of the dialkyl itaconates can replace the datively bonded THF ligand in **1**$^+$ to form the catalyst−monomer complexes or adduct intermediates **1·DMIA** and **1·D$^i$PrIA**, which rapidly undergo Michael addition via nucleophilic attack of the ester enolate ligand to form the eight-membered-ring chelates **2a**,**b**. Interestingly, monitoring the reactions by $^1$H NMR upon warming to ambient temperature and standing for 24 h revealed a slow, but clean, evolution to products **4a**,**b** as orange and red solutions, respectively. We hypothesized that such *kinetic to thermodynamic* product transformation arose from a slow ligand exchange on going from the coordinated isopropyl ester in **2a** (and **2b**) to the $\beta$-alkyl ester in **4a** (and **4b**), resulting in the shrinkage of the ring size from an eight- to seven-membered chelate structure. In addition, an associative mechanism


DOI: 10.1021/acs.organomet.7b00358
Organometallics 2017, 36, 2922−2933

**Scheme 2. Proposed Reactivity of $C_2$-Ligated Cationic *ansa*-Zirconocenium complex $1^+$ with Dialkyl Itaconates and $^{13}C$ NMR Chemical Shifts ($CD_2Cl_2$, ppm) for the Carbonyl Carbons in Kinetic Products 2a,b as well as Thermodynamic Products 4a,b[a]**

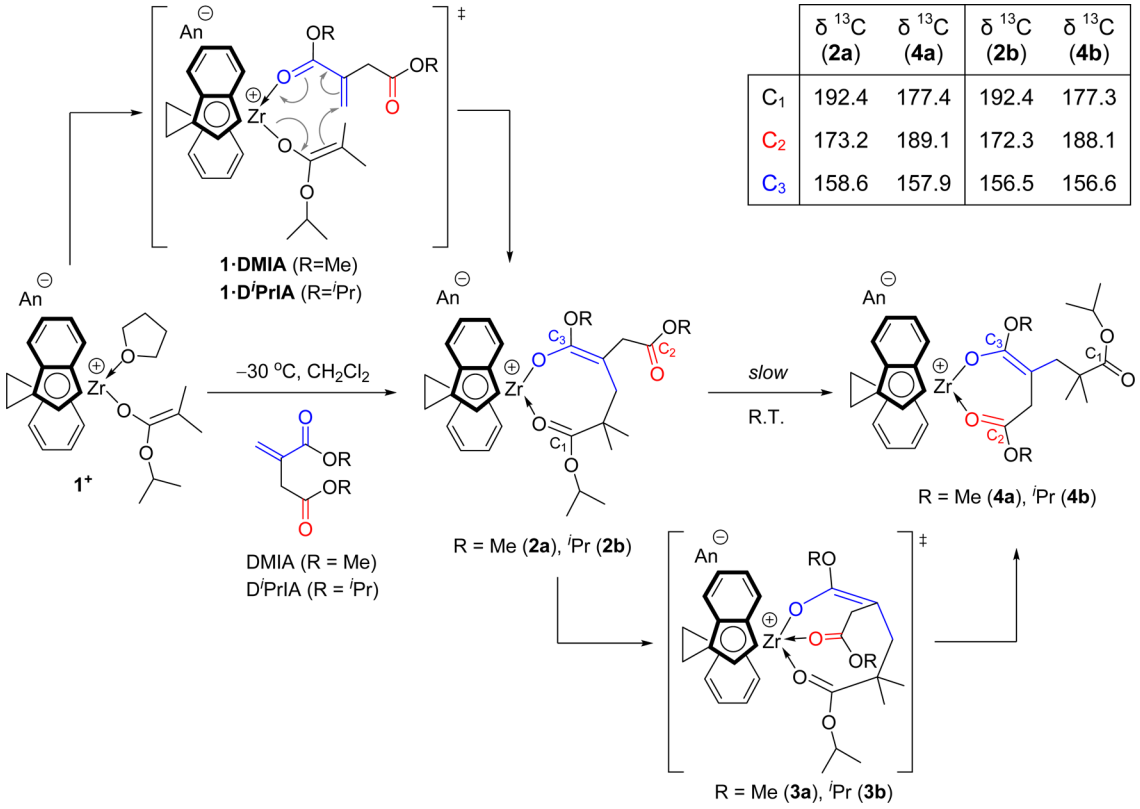


| | δ $^{13}C$ (**2a**) | δ $^{13}C$ (**4a**) | δ $^{13}C$ (**2b**) | δ $^{13}C$ (**4b**) |
|---|---|---|---|---|
| $C_1$ | 192.4 | 177.4 | 192.4 | 177.3 |
| $C_2$ | 173.2 | 189.1 | 172.3 | 188.1 |
| $C_3$ | 158.6 | 157.9 | 156.5 | 156.6 |

[a] $An^- = [MeB(C_6F_5)_3]^-$.

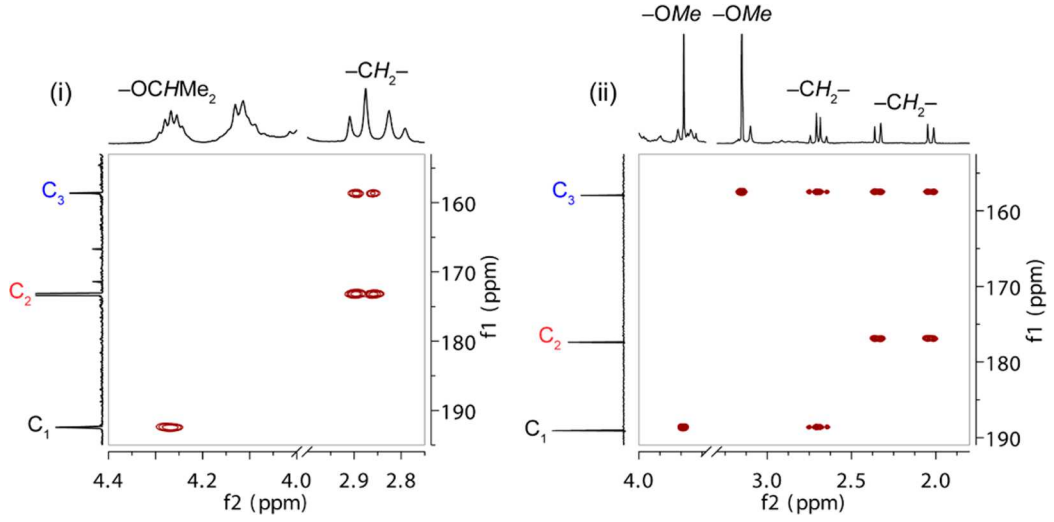


**Figure 1.** Selected portions of $^{13}C-^1H$ HMBC ($CD_2Cl_2$, −5 °C) 2D NMR spectra of complexes **2a** (i) and **4a** (ii) shown for comparison.

involving a five-coordinated Zr center (**3a,b**) was considered to be more favorable than the alternative dissociative mechanism, due to the high oxophilicity of the cationic Zr and the observed inability of the more sterically hindered Cp*($^n$PrCp)Zr system to form the seven-membered-ring chelate analogue (vide infra). Furthermore, a hypothetical dissociation of the coordinated *β*-alkyl ester in the intermediates **3a,b** would revert them back to the starting complexes **2a,b** and is nonproductive, but the successful and clean isolation of complexes **4a,b** on a preparative scale and at room temperature (see Experimental Details in the Supporting Information) suggests that the dissociation of the isopropyl ester group derived from the mono ester enolate ligand in $1^+$ was more favorable and irreversible.

The stability of complexes **2a,b** for over 24 h at −18 °C allowed their full spectroscopic characterization by $^1H$ and $^{13}C$ NMR at this temperature. Raising the temperature again above 0 °C or warmer allowed for the gradual evolution to thermodynamically more stable complexes **4a,b**, indicative of a kinetic barrier for forming five-coordinated intermediate **3**.



DOI: 10.1021/acs.organomet.7b00358
*Organometallics* 2017, 36, 2922−2933

Thus, upon addition of a stoichiometric amount of dialkyl itaconates, dissociation of the coordinated THF molecule in $\mathbf{1}^+$ was indicated by characteristic peaks at 3.66 and 1.80 ppm (for $\alpha$ and $\beta$ H atoms, respectively) in the $^1$H NMR and at 67.94 and 25.71 ppm (for $\alpha$ and $\beta$ C atoms, respectively) in the $^{13}$C NMR. Formation of complexes **2a,b** was also supported by other $^1$H NMR resonances: (1) appearance of the methylene protons (2.29 and 1.72 ppm for **2a**, 2.23 and 1.71 ppm for **2b**) derived from the consumption of the vinylic protons of DMIA and D$^i$PrIA, (2) a marked chemical downfield shift of the septet for $-$OC*H*Me$_2$ at 3.73 ppm of the isopropyl ester enolate in $\mathbf{1}^+$, to 4.27 and 4.19 ppm of the $-$OC*H*Me$_2$ now attached to the ester group in **2a,b**, respectively, (3) the alkyl ester groups in the DMIA and D$^i$PrIA showing a clear downfield shift in their $^1$H NMR spectra as they went from free itaconates (singlets at 3.73 and 3.66 ppm for the two $-$OMe in DMIA, and doublets at 1.23 and 1.20 ppm for the two $-$OCHMe$_2$ in D$^i$PrIA) to the addition products **2a** (singlets at 3.64 and 3.09 ppm for the two $-$OMe) and **2b** (doublets at 1.37 and 1.23$-$1.19 ppm for the $-$OCH*Me*$_2$), and (4) the upfield shift of >CMe$_2$ (1.19 and 1.09 ppm for **2a**, 1.13 and 0.98 ppm for **2b**). Importantly, the resonances appearing in the carbonyl region of the $^{13}$C NMR clearly suggested the presence of two types of carbonyl carbons in accordance with the open chelate structures proposed for **2a,b**. Using compound **2a** as an example, apart from the ester enolate ligand (OC(OMe)=) at 158.6 ppm ($C_3$), two carbonyl signals were observed at 173.2 ppm ($C_2$), typical of a free noncoordinated alkyl ester, and at 192.4 ppm ($C_1$), which indicates a more deshielded alkyl ester as a consequence of its coordination to the cationic Zr center (Scheme 2). The $^{13}$C$-^1$H HMBC spectra of **2a** recorded at $-5$ °C (Figure 1(i)) showed a clear correlation between the signal at 192.4 ppm and the $-$OC*H*Me$_2$ of the isopropyl ester, therefore providing further evidence for the eight-membered-ring chelate ligand structure through the coordination of the carbonyl in the [*C*(O$^i$Pr)=O] moiety as depicted in Scheme 2. All other correlations in the 2D spectrum, as well as the analogous case observed for the otherwise similar complex **2b** (Figure S40(i) in the Supporting Information), pointed to the same conclusion.

Complexes **4a,b** were also isolated on a preparative scale after stirring solutions of **2a,b**, respectively, in $CH_2Cl_2$ at room temperature for 24 h. This intriguing structural evolution on going from an eight- to a seven-membered-ring chelate structure is clearly illustrated in Figure 2, which shows the downfield shift of the resonance at 4.27 ppm, corresponding to the coordinated $-$OC*H*Me$_2$ in **2a**, to 4.89 ppm, now the free $-$OC*H*Me$_2$ in **4a**. Likewise, the $-$OC*H*Me$_2$ resonance in **2b** was also found to be shifted downfield from 4.19 ppm (coordinated) to 4.93 ppm (free) in **4b**. Other important chemical shift differences that indicated such structural evolution are (1) the shift of the alkyl ester signals in **4a** (singlets at 3.73 and 3.15 ppm for the two $-$OMe) and **4b** (doublets at 1.43, 1.23, and 0.97 ppm for the $-$OCH*Me*$_2$), (2) the upfield shift of the diastereotopic methylene protons of the pendant itaconate moiety in **2a** (doublets at 2.89 and 2.81 ppm) and **2b** (doublets at 2.89 and 2.79 ppm), now part of the seven-membered ring chelate ligand in **4a** (doublets at 2.73 and 2.67 ppm) and **4b** (doublets at 2.70 and 2.65 ppm), and (3) the slight shift of the >CMe$_2$ (1.12 and 1.06 ppm for **4a**, 1.14 and 1.09 for **4b**), now part of the pendant alkyl chain. More importantly, the marked chemical shift differences in the carbonyl region of the $^{13}$C NMR spectra, recorded at room

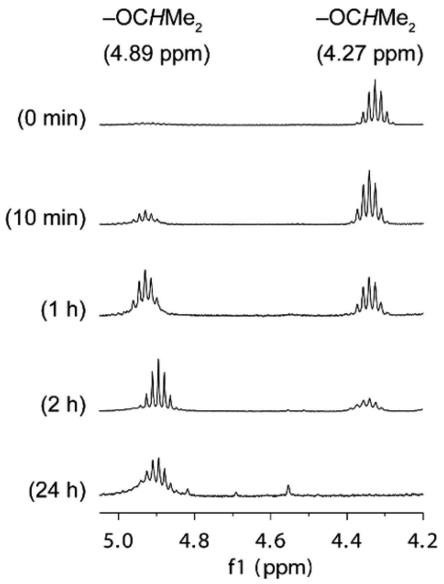


**Figure 2.** Time evolution of the $-$OC*H*Me$_2$ region of the $^1$H NMR spectrum ($CD_2Cl_2$, 25 °C) of **2a** in $CD_2Cl_2$ at ambient temperature.

temperature (Scheme 2), provided corroborative evidence for the proposed seven-membered-ring structures **4a,b**. Using compound **4a** as an example, the ester enolate ligand [OC(OMe)=] remained almost constant at 157.9 ppm ($C_3$), as its pivotal position did not change from **2a** to **4a**; however, the resonance at 177.4 ppm ($C_1$), typical of a noncoordinated alkyl ester, now belongs to the free isopropyl ester [*C*(O$^i$Pr)=O], formerly coordinated to the Zr in **2a**, while the much deshielded resonance at 189.1 ppm ($C_2$) corresponds to the $\beta$-methyl ester [*C*(OMe)=O], now coordinated to the cationic Zr center. Similarly for **4b**, a signal at 156.6 ppm ($C_3$) is assigned for the coordinated ester enolate [OC(O$^i$Pr)=], a signal at 177.3 ppm ($C_1$) for the free isopropyl ester [*C*(O$^i$Pr)=O], formerly coordinated to Zr, and a signal at 188.1 ppm ($C_2$) for the coordinated $\beta$-isopropyl ester [*C*(O$^i$Pr)=O]. These assignments were supported by the correlations observed in the $^1$H$-^{13}$C HMBC experiments, as shown in Figure 1(ii) and Figure S40(ii) in the Supporting Information.

On the basis of the stoichiometric reactions described above, coupled with control experiments in which extra amounts of DMIA, D$^i$PrIA, and MMA were added to preformed complexes **2a,b** and **4a,b** showing no monomer conversion, we concluded that the lack of polymerization activity of $\mathbf{1}^+$ toward dialkyl itaconates was due to the inability of the first monomer-addition product to further enchain the incoming monomer molecules. Furthermore, we monitored the addition of 2 equiv of MMA to complexes **2a,b** by $^1$H NMR and observed no apparent interaction, followed by the identical evolution previously observed into complexes **4a,b**. These results indicate that the incoming monomer molecules are incapable of ring opening the eight- or seven-membered ring chelate to enter the coordination site, thus precluding subsequent Michael additions for chain growth.

**Reactivity of $C_2$-Ligated Bridged *ansa*-Zirconocene Complexes with Itaconic Anhydride.** Next, we investigated the reactivity of complex $\mathbf{1}^+$ with 1 equiv of IA (Scheme 3). Upon mixing, the red solution of $\mathbf{1}^+$ turned yellow and an intractable mixture was observed by $^1$H NMR; even at $-80$ °C no clean product was observed. Furthermore, the color change


DOI: 10.1021/acs.organomet.7b00358
*Organometallics* 2017, 36, 2922−2933

**Scheme 3. Reactivity of Neutral *ansa*-Zirconocene Complex 1 and Cationic $1^+$ with Itaconic Anhydride (IA) and $^{13}C$ NMR Chemical Shifts ($CD_2Cl_2$, ppm) for the Carbonyl Carbons in Products 5 and 7**[a]

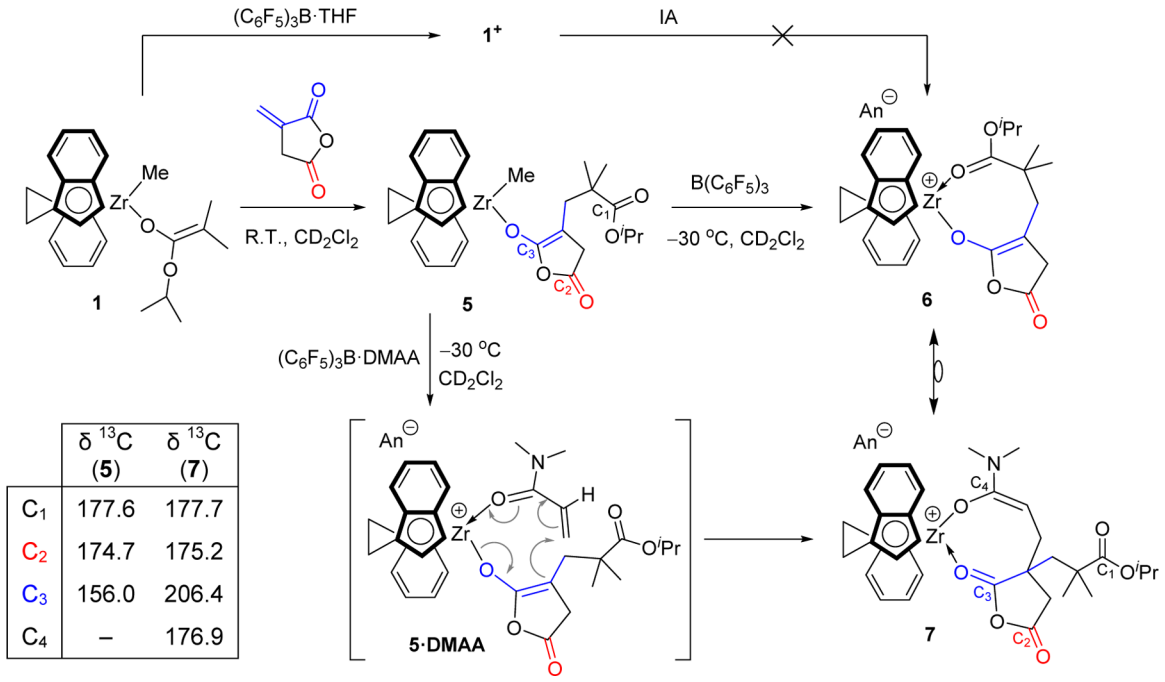


| | δ $^{13}C$ (**5**) | δ $^{13}C$ (**7**) |
|---|---|---|
| $C_1$ | 177.6 | 177.7 |
| $C_2$ | 174.7 | 175.2 |
| $C_3$ | 156.0 | 206.4 |
| $C_4$ | – | 176.9 |

[a] $An^- = [MeB(C_6F_5)_3]^-$.

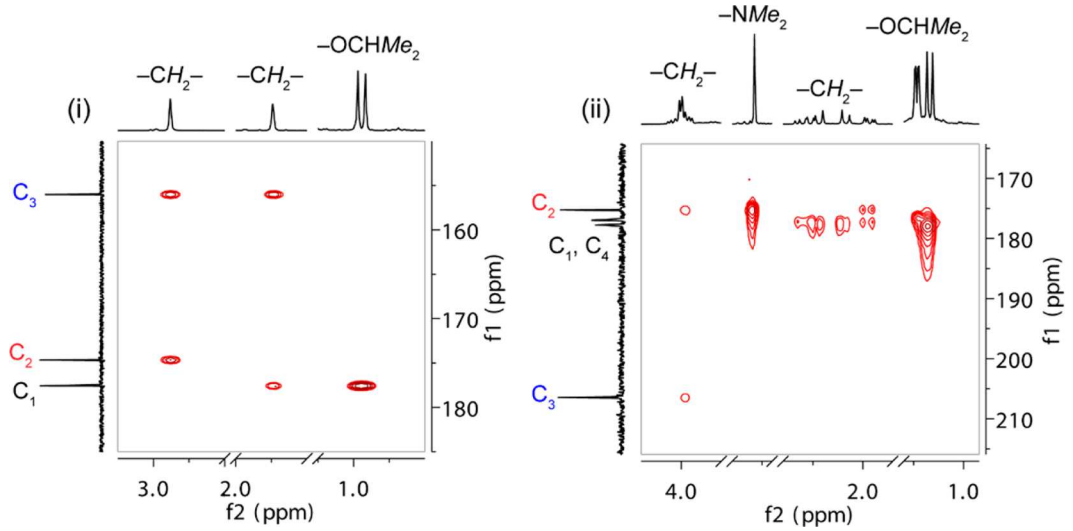


**Figure 3.** Selected portions of $^{13}C-^1H$ HMBC ($CD_2Cl_2$, 25 °C) 2D NMR spectra of complexes **5** (i) and **7** (ii).

was followed by rapid decomposition, preventing any further product identification. We hypothesized that the formation of the direct addition product of $\mathbf{1}^+$ and IA, represented by unstable complex **6** (vide infra), was unfavorable due to the intrinsic ring strain that the internal $sp^2$-hybridized C═C in the cyclic enolate anhydride exerted over the eight-membered-ring chelate structure, resulting from the coordination of the isopropyl ester to the cationic Zr center. It is also possible that the THF molecule present in the reaction mixture partially displaced the chelate oxygen of the isopropyl ester to release the chelate ring strain. This high-ring-strain phenomenon would also explain the inability of complex $\mathbf{1}^+$ to polymerize IA, since an eight-membered-ring structure, containing an strained cyclic enolate anhydride, would be required for a monometallic coordination–addition polymerization analogous to the polymerization of other acrylic monomers. In contrast, structurally comparable α-methylene-γ-butyrolactones (MBLs), which consist of a five-membered-ring lactone only lacking one carbonyl oxygen, can be readily polymerized by cationic $\mathbf{1}^+$ by a monometallic site-controlled mechanism.[21] A unimetallic coordination–addition mechanism was also observed in the polymerization of MBLs by *ansa*-half-sandwich rare-earth-metal catalysts,[31] but a bimetallic mechanism was found for the neutral samarocene(II) complex $Cp^*_2Sm(THF)_2$.[32]

Interestingly, we found that neutral *ansa*-zirconocene methyl ester enolate **1** reacts with one molecule of IA to cleanly form the single-addition product **5** (Scheme 3). The reaction occurred rapidly at ambient temperature and in a polar



DOI: 10.1021/acs.organomet.7b00358
*Organometallics* 2017, 36, 2922–2933

**Scheme 4. Synthetic Route to Neutral and Cationic Complexes of Cp*("PrCp)Zr**

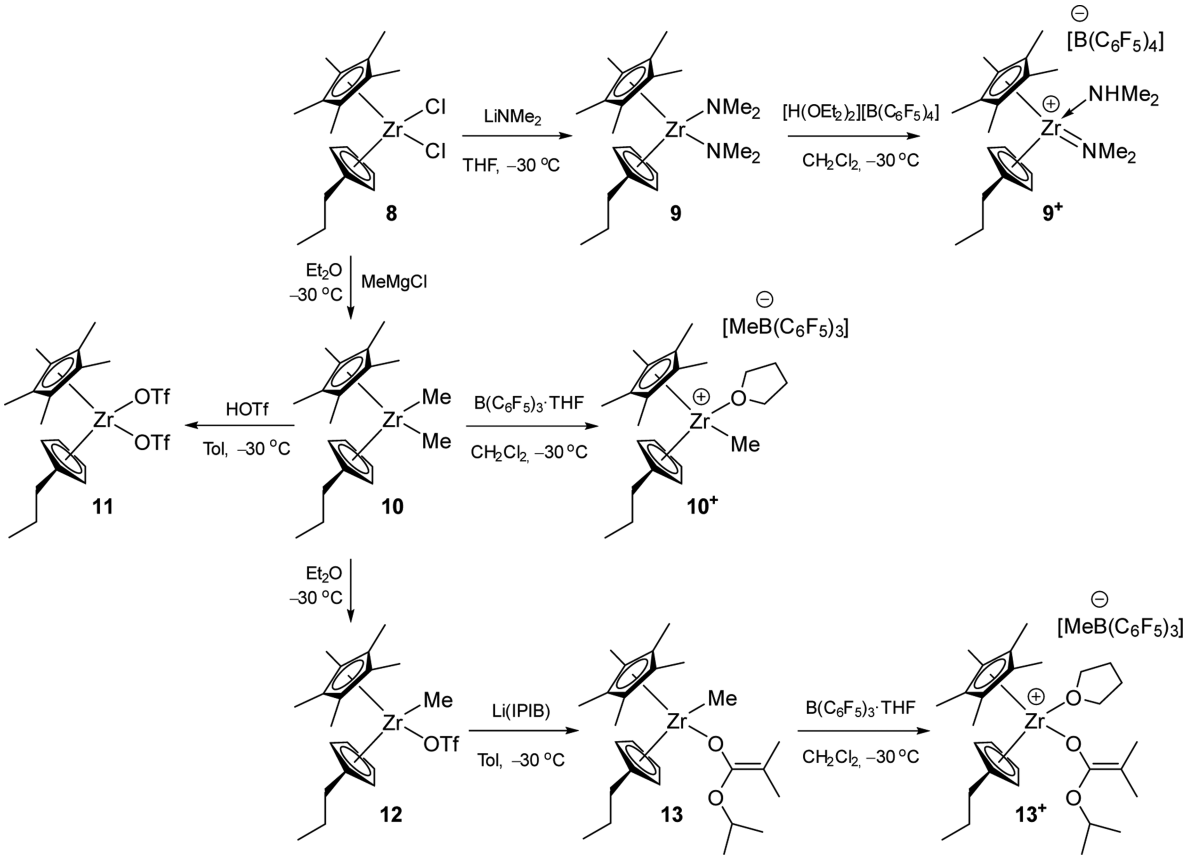


noncoordinating solvent ($CH_2Cl_2$), in a fashion analogous to that between **1** and MMA.[19] Not surprisingly, neutral complex **5** did not add more amounts of IA and thus there was no chain propagation. Complex **5** is stable in solution at room temperature for several days, presumably due to the unstrained cyclic enolate anhydride, enabled by the lack of coordination of the isopropyl ester group to the Zr, which is already coordinatively saturated with a methyl ligand. Several attempts to grow single crystals suitable for X-ray crystallography were unsuccessful, but key features in the $^1H$ and $^{13}C$ NMR spectra of the isolated product provided clear evidence to support the proposed structure of **5**: (1) the downfield shift of the septet at 3.65 ppm for $-OCHMe_2$ of the isopropyl ester enolate in **1** to 4.89 ppm of the $-OCHMe_2$ now attached to the ester group in **5**, (2) the markedly upfield shift of the methylene protons in the IA ring from 3.62 ppm of the free monomer to 2.95 ppm in **5**, (3) a new sharp singlet at 1.90 ppm for the methylene protons resulting from the vinyl addition, (4) the two inequivalent $-OCHMe_2$ in **1** (doublets at 1.01 and 0.94 ppm) now a single doublet at 1.19 ppm in **5**, and (5) the shift of the $>CMe_2$ (from 1.40 and 1.17 ppm in **1** to 0.99 and 0.97 ppm in **5**) and the −Me ligand (from −0.96 ppm in **1** to −0.85 ppm in **5**). Altogether, the chemical resonances observed in the carbonyl region of the $^{13}C$ NMR spectrum, typical of free alkyl esters, were also consistent with an open structure in which both oxygen atoms of the akyl (177.6 ppm for $[C(O^iPr)=O]$, $C_1$) and anhydride ester groups (174.7 ppm for $[CH_2C(O)=O]$, $C_2$) are not coordinated to the Zr center, as shown in the $^{13}C-^1H$ HMBC spectrum (Figure 3(i)).

Subsequently, we examined the activation of complex **5** with 1 equiv of $B(C_6F_5)_3$ in $CD_2Cl_2$ at −30 °C, aiming for the formation and stabilization of the corresponding cationic complex **6** through the coordination of the isopropyl ester group in the absence of an external donor such as THF. Indeed, complex **6** was observed by $^1H$ and $^{19}F$ NMR (Figure S11 in the Supporting Information), but it rapidly decomposed at room temperature in less than 20 min, precluding its isolation and further characterization. Interestingly, the existence of two broad signals at 4.94 and 4.36 ppm for the $-OCHMe_2$, with an combined integral value of 1 H, together with broad singlets for the methylene protons in the cyclic anhydride (3.36 ppm) and the eight-membered-ring chelate (2.00 ppm), suggested a dynamic behavior on the $^1H$ NMR time scale at this temperature, presumably due to the ring strain caused by the $sp^2$ hybridization in the cyclic enolate anhydride. Nevertheless, the clean methyl abstraction by $B(C_6F_5)_3$ was confirmed in the $^1H$ NMR spectrum of **6** by the disappearance of the methyl signal in **5** (−0.85 ppm) and the appearance of a characteristic broad peak at 0.49 ppm in **6** for the resulting uncoordinated anion $[MeB(C_6F_5)_3]^-$, also supported by the $^{19}F$ NMR by resonances at −133.03 (d, *o*-F), −165.09 (t, *p*-F), and −167.71 ppm (m, *m*-F). Other significant signals in the $^1H$ NMR to support structure **6** are a sharp singlet for the ethylene bridge at 4.12 ppm, two doublets for the diasterotopic isopropyl groups at 1.37 and 1.33 ppm, and two singlets for the two $>CMe_2$ at 1.30 and 1.25 ppm.

The above experimental results led to a hypothesis that, if the instability of complex **6** to form an eight-membered-ring chelate structure originates from the ring strain of the enolate anhydride, then subsequent regeneration of the anhydride should be favorable, as it releases the chelate strain. To this end, concomitant activation of neutral enolate anhydride **5** and



DOI: 10.1021/acs.organomet.7b00358
*Organometallics* 2017, 36, 2922−2933

addition of a monomer with stronger basicity, such as dimethyl acrylamide (DMAA), should undergo Michael addition through an intermediate, **5·DMIAA**, in which the DMAA occupies the open coordination site and prevents a strained chelate analogous to **6**. Indeed, addition of the $(C_6F_5)_3B$·DMAA adduct in stoichiometric amount to **5** cleanly formed the much less strained amide ester enolate **7** with regeneration of the cyclic anhydride. As we expected, complex **7** was more stable in solution at room temperature, thus allowing for its full 1D $^1H$, $^{19}F$, $^{13}C$ NMR and 2D $^1H-^{13}C$ HMBC NMR analysis before its degradation. Clean abstraction of the methyl group in **5** and formation of the anion $[MeB(C_6F_5)_3]^-$ was once again observed by the $^1H$ (broad singlet at 0.51 ppm) and $^{19}F$ NMR spectra. Other notable features in the $^1H$ NMR spectra of **7** include (1) the downfield shift of the methylene protons of the cyclic anhydride from 2.95 ppm in **5** to 3.98 ppm in **7**, (2) two sharp singlets for the $NMe_2$ at 3.26 and 2.79 ppm, (3) a new doublet for the C=C*H* of the amide ester enolate at 2.52 ppm, (4) a set of diasterotopic methylene protons for $-CH_2-$ in the chelate ring and the noncoordinated alkyl chain between 2.29 and 1.96 ppm, and (5) a clear shift of the isopropyl ester groups (doublets at 1.24 and 1.23 ppm) and the $>CMe_2$ (1.18 and 1.15 ppm). Altogether, analysis of the $^{13}C$ NMR spectrum of **7** revealed a set of four carbonyl C atoms supporting the eight-membered-ring chelate structure depicted in Scheme 3, whose assignment was corroborated by the $^1H-^{13}C$ HMBC spectrum (Figure 3(ii)): a coordinated amide ester enolate $[OC(NMe_2)=]$ at 176.9 ppm ($C_4$), two noncoordinated alkyl esters at 177.7 ppm ($C_1$) of the isopropyl $[C(O^iPr)=O]$ and at 175.2 ppm ($C_2$) of the cyclic anhydride $[CH_2C(O)=O]$, and finally a very deshielded carbonyl carbon of the coordinated cyclic anhydride at 206.4 ppm ($C_3$), thus confirming the transformation of the cyclic anhydride enolate in **5**.

**Reactivity of Unbridged Zirconocene Complexes with Dialkyl Itaconates and Itaconic Anhydride.** To examine the possible *ansa* effects on the reactivity of zirconocene complexes with itaconates and IA, we next synthesized unbridged zirconocene complexes and subsequently investigated their reactivity toward such substrates.

We initially examined the dichloride complex of the unbridged, more sterically encumbered Cp*($^n$PrCp)$ZrCl_2$ (**8**; Cp*($^n$PrCp) = ($\eta^5$-pentamethylcyclopentadienyl)($\eta^5$-*n*-propylcyclopentadienyl)) for steric protection of the Zr center and solubility reasons. The crystalline bis(amido) complex Cp*($^n$PrCp)$Zr(NMe_2)_2$ (**9**; Scheme 4) was obtained by treating dichloride complex **8** with 2 equiv of $LiNMe_2$. Reaction of **9** with 1 equiv of Jutzi's salt, $[H(OEt_2)_2][B(C_6F_5)_4]$, at −30 °C produced the cationic complex $[Cp^*(^nPrCp)Zr(HNMe_2)=NMe_2]^+[B(C_6F_5)_4]^-$ (**9**$^+$), stabilized by the released coproduct dimethylamine (Scheme 4). The structure was confirmed by $^1H$ and $^{13}C$ NMR and X-ray crystal analysis (Figure 4 and Figure S16 and S17 in the Supporting Information).

Scheme 4 outlines the procedure for obtaining neutral monoester enolate zirconocene complex **13** and the generation of the corresponding cationic complex Cp*($^n$PrCp)Zr(THF)$[OC(O^iPr)=CMe_2]^+[MeB(C_6F_5)_3]^-$ (**13**$^+$), which was inspired by the efficient formation of neutral monoester enolate complexes of $C_2$- and $C_s$-ligated *ansa*-zirconocenes.[33] Thus, dichloride **8** was conveniently converted into the dimethyl derivative Cp*($^n$PrCp)$ZrMe_2$ (**10**) with MeMgCl and subsequently transformed into the methyl triflate Cp*($^n$PrCp)Zr(OTf)Me (**12**) by means of $Me_3SiOTf$. Alternatively, treatment of dimethyl **10** with 2 equiv of triflic acid quantitatively

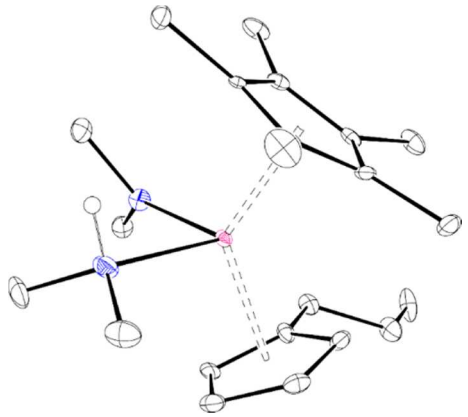

**Figure 4.** X-ray crystal structure of $[Cp^*(^nPrCp)Zr(HNMe_2)=NMe_2]^+[B(C_6F_5)_4]^-$ (**9**$^+$), with thermal ellipsoids drawn at 30% probability (the $[B(C_6F_5)_4]^-$ anion was omitted for clarity).

generated the bis(triflate) complex Cp*($^n$PrCp)$Zr(OTf)_2$ (**11**). Reaction of **11** with 2 equiv of $Li[OC(O^iPr)=CMe_2]$ failed to form the diester enolate derivative, attributable to the sterics of the intended bis(enolate) complex, and mixtures of monosubstituted products were obtained instead. On the other hand, methyl triflate **12** reacted cleanly with 1 equiv of $Li[OC(O^iPr)=CMe_2]$ to afford the methyl zirconocene ester enolate **13**. Characteristic $^1H$ signals in the NMR spectrum include the septet at 4.07 ppm for the methine proton in $-OCHMe_2$, the two doublets centered at 1.19 ppm for the two diasterotopic $-OCHMe_2$, and two singlets at 1.88 and 1.66 ppm for the two isopropylidene methyl groups.

Reaction of **13** with $(C_6F_5)_3B$·THF was instantaneous, leading to the corresponding cationic complex **13**$^+$ quantitatively at low or ambient temperature in $CH_2Cl_2$. The abstraction of the methyl ligand was observed in the $^1H$ NMR (Figure S28 in the Supporting Information) by a dramatic shift from a sharp singlet at 0.15 ppm in **13** to a broad signal at 0.49 ppm in **13**$^+$, typical of the uncoordinated counterion $[MeB(C_6F_5)_3]^-$; the coordination of the THF molecule was clearly indicated by the chemical shifts at 4.16–4.02 and 2.17 ppm (for $\alpha$-$CH_2$ and $\beta$-$CH_2$, respectively), shifted downfield with respect to the free THF (3.66 and 1.80 ppm). Similarly to **13**, the dimethyl species **10** was activated by $(C_6F_5)_3B$·THF to form the cationic complex $[Cp^*(^nPrCp)Zr(THF)Me]^+[MeB(C_6F_5)_3]^-$ (**10**$^+$, Scheme 4). The $^1H$ NMR spectral differences between the neutral and the cationic species are similar to those of **13** and **13**$^+$, with the most notable being the shift of the resonance at −0.35 ppm of the two methyl groups in **10** to a broad signal at 0.48 ppm in **10**$^+$ and the two resonances of the Cp protons in the symmetrically substituted **10** (5.71 and 5.35 ppm) being split into four resonances in the now unsymmetrically substituted **10**$^+$ (6.25, 6.03, 5.90, and 5.79 ppm).

With the unbridged cationic zirconocenium complexes on hand, we subsequently examined their ability to polymerize DMIA, D$^i$PrIA, and IA and found that cationic dimethylamido **9**$^+$, methyl **10**$^+$, and ester enolate **13**$^+$ produced no polymer products up to 24 h at room temperature (in $CH_2Cl_2$) or 100 °C (in $C_6H_5Br$). Only complex **9**$^+$ showed some catalytic activity in isomerization of DMIA and D$^i$PrIA (50 equiv) into the corresponding dimethyl and diisopropyl citraconates, respectively. A bimolecular polymerization pathway, known to be well controlled in the polymerization of MMA by two-


DOI: 10.1021/acs.organomet.7b00358
Organometallics 2017, 36, 2922–2933

component unbridged $Cp_2Zr$-type systems,[34−36] was also employed by activating only 1/2 equiv of **9**, **10**, and **13** with $[H(OEt_2)_2][B(C_6F_5)_4]$ or $(C_6F_5)_3B{\cdot}THF$ to generate the corresponding neutral/cationic complex mixtures **9**/**9**$^+$, **10**/**10**$^+$, and **13**/**13**$^+$ in 1/1 ratios; they too produced no polymer products.

To seek insight into the lack of the polymerization activity of such cations, we investigated the stoichiometric reactions between the cations and the monomer. First, the reaction of **9**$^+$, **10**$^+$, and **13**$^+$ with 1 equiv of IA at −30 °C was followed by NMR, revealing in all cases instantaneous decomposition products. Attempts to detect any clean addition products at −80 °C were also unsuccessful. Second, we surveyed the reactivity of the dialkyl itaconates with cationic amido zirconocene **9**$^+$. NMR-scale reactions between **9**$^+$ and 1 equiv of DMIA or D$^i$PrIA at −30 °C showed intractable mixtures of products, including partial formation of dialkyl citraconates. Third, we examined the stoichiometric reaction between **10**$^+$ and 1 equiv of dialkyl itaconates at −30 °C. Key chemical shift differences in both the $^1$H and $^{13}$C NMR spectra (Figures S30 and S32 in the Supporting Information) pointed to a ligand exchange between the coordinated THF and the dialkyl itaconates to form itaconate adducts **14a,b** (Scheme 5), with no signs of methyl addition to the coordinated monomer.

**Scheme 5. Reactivity of Cationic Complex 10$^+$ with Dialkyl Itaconates**[a]

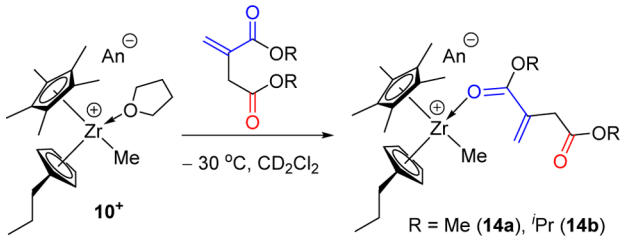


[a]$An^- = [MeB(C_6F_5)_3]^-$.

Next, we investigated the stoichiometric reactions between the in situ generated monoester enolate **13**$^+$ and 1 equiv of the dialkyl itaconates. The reaction at −30 °C proceeded cleanly and produced eight-membered chelating complexes **15a,b** (Scheme 6) as a result of the fast conjugated Michael addition of the ester enolate ligand to the conjugated C═C double bond of the coordinated monomers DMIA and D$^i$PrIA, via the proposed catalyst−monomer complexes or intermediates **13**·**DMIA** and **13**·**D$^i$PrIA**, respectively. However, in sharp contrast to the reactivity observed with $C_2$-ligated *ansa*-zirconocene complexes **2a,b** (vide supra), species **15a,b** are stable in solution at room temperature and undergo no evolution via ligand exchange between the two available carbonyl oxygens (i.e., conversion from the eight-membered-ring to the seven-membered-ring chelate structures **16a,b**, Scheme 6), up to 24 h or under heating. We attributed the observation that the sterically crowded Zr centers in **15a,b** do not undergo such transformation due to the smaller bite angle and the higher steric hindrance of the Cp*($^n$PrCp) ligand system, further supporting our former hypothesis that a stererically demanding five-coordinated intermediate is required on going from the eight-membered-ring chelate to the seven-membered-ring species.

The formation of the single monomer addition products was clearly indicated by the $^1$H NMR spectra, which showed complete and rapid consumption of the vinylic resonances of the conjugated C═C in the dialkyl itaconates, accompanied by formation of diasteromeric methylene signals at 2.64 and 1.84 ppm in **15a** and at 2.64 and 1.90 ppm in **15b**. Moreover, the septet at 4.02 ppm for $-OCHMe_2$ of the coordinated isopropyl ester enolate group ($^{13}$C resonance at 154.9 ppm for [OC(O$^i$Pr)═]) in **13**$^+$ was shifted markedly downfield to 4.96 and 4.98 ppm (for **15a,b**, respectively) for the $-OCHMe_2$ of the now coordinated isopropyl ester group (new $^{13}$C resonances at 193.8 and 193.7 ppm for [C(O$^i$Pr)═O] in **15a,b**, respectively). The assignment of the carbonyl resonances in the $^{13}$C NMR was supported by 2D $^1$H−$^{13}$C HMBC experiments recorded at room temperature in $CD_2Cl_2$ (Figure 5). For

**Scheme 6. Reactivity of Cationic Complex 13$^+$ with Dialkyl Itaconates**[a]

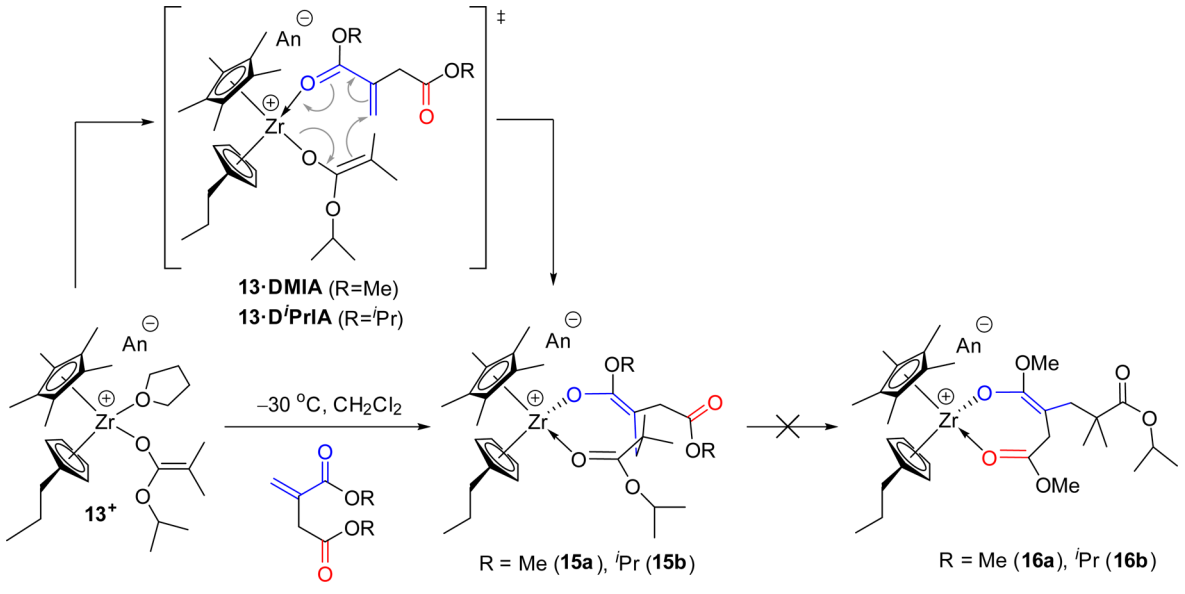


[a]$An^- = [MeB(C_6F_5)_3]^-$.



DOI: 10.1021/acs.organomet.7b00358
Organometallics 2017, 36, 2922−2933

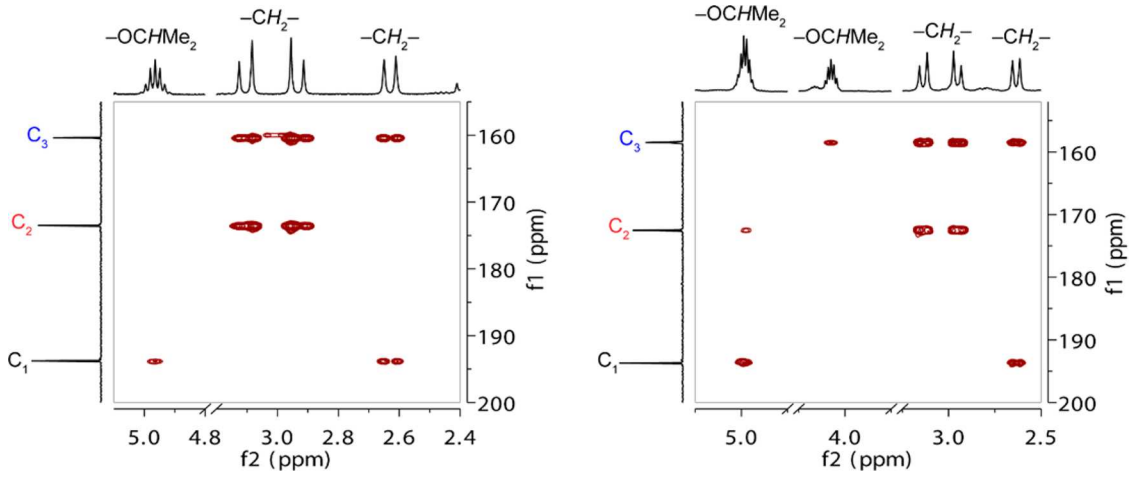


**Figure 5.** Selected portions of $^{13}C-^{1}H$ HMBC ($CD_2Cl_2$, 25 °C) 2D NMR spectra of complexes **15a** (left) and **15b** (right) shown for comparison.

instance, the resonances observed at 173.5 and 172.5 ppm, chemical shifts which are typical of those of free alkyl ester carbonyl carbons, showed strong correlations with the diasterotopic protons of the vicinal methylene group at 3.10 and 2.93 ppm for **15a** and at 3.14 and 2.95 ppm for **15b**. These observations led to the conclusion that the noncoordinated carbonyl signals indeed corresponded to the *β*-alkyl ester carbonyl carbons originated from the dialkyl itaconates.

Again, control experiments showed no further consumption of excess DMIA, D$^{i}$PrIA, or MMA. Thus, the lack of polymerization activity of **13**$^{+}$ toward dialkyl itaconates can be attributed to the inability of the incoming monomer to enter the coordination sphere of the Zr center in the preformed eight-membered-ring chelate complexes **15a,b**, thus preventing further chain growth.

As in the case of $C_2$-ligated *ansa*-zirconononocene complex **1**, unbridged neutral methyl ester enolate zirconocene **13** reacts with IA instantaneously to generate cleanly the corresponding single monomer addition product **17** (Scheme 7). The

**Scheme 7. Reactivity of Neutral Zirconocene Complex 13 with Itaconic Anhydride**

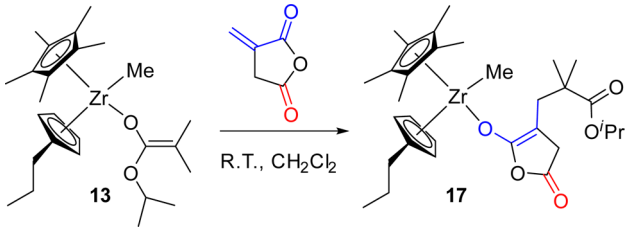


generation of the cyclic enolate anhydride was evidenced by key resonances observed in the $^{1}H$ and $^{13}C$ NMR spectra, including (1) the complete disappearance of the vinylic protons of IA and appearance of new methylene protons (sharp singlet at 2.11 ppm), (2) the marked downfield shift of the septet for $-OCHMe_2$ at 4.07 ppm of the isopropyl ester enolate in **13** to 4.92 ppm of the $-OCHMe_2$ now attached to the ester group in **17**, (3) the upfield shift of the $>CMe_2$ (1.07 and 1.05 ppm) and the methyl ligand (−0.06 ppm), and (4) only one doublet for the isopropyl group (1.21 ppm). In addition, the resonances corresponding to the carbonyl carbons in the $^{13}C$ NMR spectrum of isolated complex **17** at 177.7 ppm for the [*C*(O)=O] of the cyclic anhydride and at 174.9 ppm for the [*C*(O$^{i}$Pr)=O] of the isopropyl ester are typical of that of free noncoordinated carbonyl esters, indicative of the open chain structure as depicted in Scheme 7, in which the terminal isopropyl ester group is not coordinated to the metal center.

**Reactivity of Zr-Itaconate Chelates toward Acrylic Monomers.** It has been well established that coordination−addition polymerization of polar vinyl monomers by cationic zirconocenium catalysts occurs through a labile eight-membered-ring chelate intermediate (resting state, exemplified by **B** in Scheme 8) formed upon Michael addition of the

**Scheme 8. Monometallic Coordination−Addition Polymerization Mechanism of DMAA by Zr-Itaconate Chelates 2a,b and 15a,b**[a]

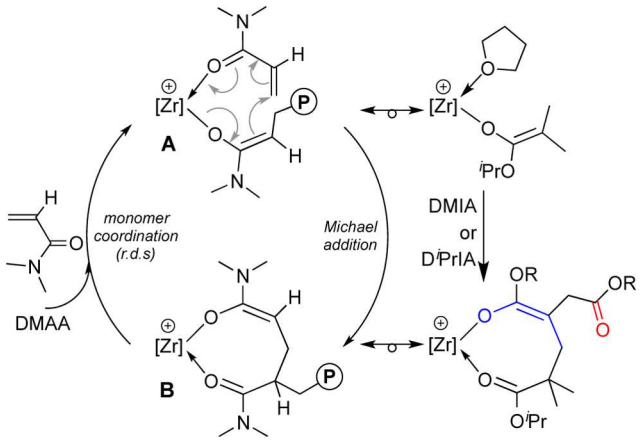


[a][Zr] = [*rac*-(EBI)]Zr, [Cp*(*n*PrCp)]Zr, paired with $[MeB(C_6F_5)_3]^{-}$ as the counterion.

growing ester enolate chain end onto the conjugated C=C of the incoming monomer (active species, exemplified by **A** in Scheme 8).[18−20,23−25,27,28,32,37−40] Moreover, it has been determined that the ring opening of the resting state to accommodate the coordination of the new incoming monomer is the rate-determining step (rds) of the polymerization reaction. In this work, we have shown that DMIA, D$^{i}$PrIA, and MMA were not capable of ring opening the eight- and seven-membered-ring chelate complexes formed after the first monomer addition took place, effectively prohibiting the polymerization reaction. Furthermore, our synthetic and



DOI: 10.1021/acs.organomet.7b00358
*Organometallics* 2017, 36, 2922−2933

**Table 1. Results of DMAA Polymerization by Zr-Itaconate Catalysts**[a]

| run no. | catalyst | monomer | time (h) | conv.[b] (%) | $M_n$[c] (kg/mol) | $Đ$[c] | $I^*$[d] (%) | [*mm*][e] (%) | [*mr*][e] (%) | [*rr*][e] (%) |
|---|---|---|---|---|---|---|---|---|---|---|
| 1 | **2a** | DMAA | 0.5 | 100 | 14.9[f] | nd | 102 | >99 | | |
| 2 | **2b** | DMAA | 0.5 | 100 | 24.6[f] | nd | 61 | >99 | | |
| 3 | **15a** | DMAA | 24 | 100 | 20.1 | 1.19 | 75 | nd | nd | nd |
| 4 | **15b** | DMAA | 24 | 100 | 20.0 | 1.14 | 76 | nd | nd | nd |

[a]Conditions: solvent ($CH_2Cl_2$) 3 mL; ambient temperature (~23 °C); $[M]_0/[catalyst]_0$ = 150. nd = not determined. [b]Monomer (M) conversion measured by $^1$H NMR. [c]Number-average molecular weight ($M_n$) and dispersity ($Đ$) determined by gel-permeation chromatography (GPC) relative to PMMA standards. [d]Initiator efficiency ($I^*$) = $M_n$(calcd)/$M_n$(exptl), where $M_n$(calcd) = MW(M) × $[M]_0/[catalyst]_0$ × conversion % + MW of chain-end groups. [e]Tacticity measured by $^1$H NMR in $CDCl_3$. [f]Calculated by $^1$H NMR.

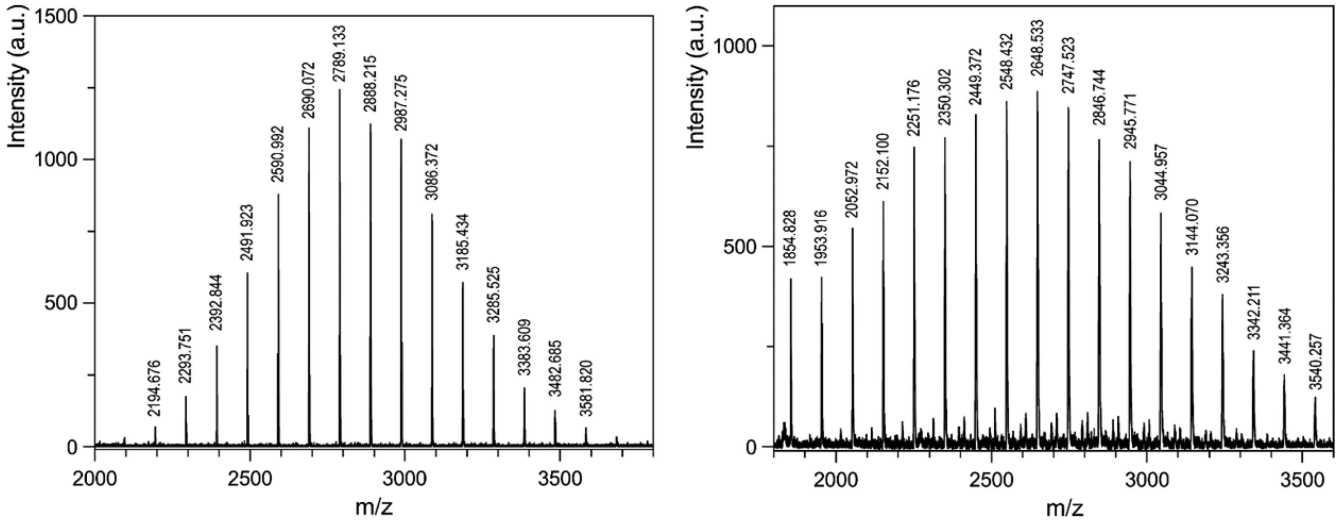


**Figure 6.** Portion of the MALDI-TOF mass spectrum of the low-molecular-weight PDMAA produced by **2a** (left) and **2b** (right) at 23 °C in $CH_2Cl_2$.

mechanistic studies with two cationic mono ester enolate zirconocenium complexes, $C_2$-ligated *ansa*-metallocenium $\mathbf{1}^+$ and unbridged metallocenium $\mathbf{13}^+$, suggested that the basicity of the conjugated carbonyl oxygen in the incoming monomer must be high enough so that displacement of the chelating carbonyl ester can occur; subsequent fast Michael addition of the enolate polymer chain end would propagate the polymerization reaction. Accordingly, we hypothesized that a highly basic acrylamide monomer, such as DMAA,[23] should be capable of ring opening Zr-itaconate eight- and seven-membered-ring chelates **2a**,**b** and **15a**,**b** and thus promote the DMAA polymerization.

Control experiments were first performed with newly synthesized unbridged cationic complexes dimethyl $\mathbf{10}^+$ and mono ester enolate $\mathbf{13}^+$ for the polymerizations of MMA and DMAA in order to assess their polymerization behavior (Table S1 in the Supporting Information). Polymerization of MMA by catalysts $\mathbf{10}^+$ and $\mathbf{13}^+$ produced syndiotactic-enriched PMMA in a well-controlled fashion, achieving quantitative conversion in 24 h; the PMMA produced had unimodal and narrow molecular weight distribution with $M_n$ = 13.8−17.5 kg/mol, $Đ$ = 1.20−1.21, and initiator efficiency $I^*$ = 86−109%. The similarity found between both catalytic systems indicated a similarly efficient initiation reaction promoted by the nucleophilic attack of the methyl ligand and the enolate ($OC(O^iPr)=CMe_2$) in $\mathbf{10}^+$ and $\mathbf{13}^+$, respectively. On the other hand, the polymerization of DMAA by $\mathbf{10}^+$ and $\mathbf{13}^+$ was much faster, achieving quantitative conversions in 3 and 1 h, respectively. However, important differences in the initiation rate vs propagation rate were observed between catalyst $\mathbf{10}^+$ (bimodal distribution) and catalyst $\mathbf{13}^+$ (unimodal distribution with narrow $Đ$), indicating that the more coordinating and much more reactive DMAA was highly susceptible to differences in the nucleophilic character of the initiating ligand (methyl vs enolate).

Next, eight-membered-ring Zr-itaconate chelates **2a**,**b** and **15a**,**b** were employed for polymerizations of MMA and DMAA. While **2a**,**b** exhibited no activity toward MMA polymerization, they initiated rapid polymerization of DMAA (entries 1 and 2, Table 1), achieving full conversion in 30 min. The polymerization activity of **15a**,**b** was noticeably lower, requiring 24 h to achieve quantitative monomer conversion, but the polymerization was well controlled, producing PDMAA with $M_n$ close to the theoretical value and low $Đ$ values of 1.14−1.19 (entries 3 and 4). It is worth noting here that neither MMA nor DMAA could be efficiently polymerized by seven-membered-ring chelates **4a**,**b**, highlighting *the importance of the labile eight-membered-ring chelate as the reactive propagating intermediate*, as it can be ring-opened for further monomer enchainment. In contrast, seven-membered-ring chelates, which are more thermodynamically stable isomers, cannot undergo ring-opening events, even with highly basic acrylamide monomers, therefore rendering them inactive for polymerization.

Further analysis of the $^1$H NMR of the isolated highly isotactic PDMAA obtained by **2a**,**b** allowed for identification of their polymer end groups (Figure S44 in the Supporting Information). The minor resonances at ~3.5 ppm (singlets, −O*Me*) and ~4.7 ppm (sept, −OC*H*$Me_2$), with integrals matching well with the expected polymer molecular weight, confirmed the presence of a dimethyl or diisopropyl ester at the


DOI: 10.1021/acs.organomet.7b00358
*Organometallics* 2017, 36, 2922−2933

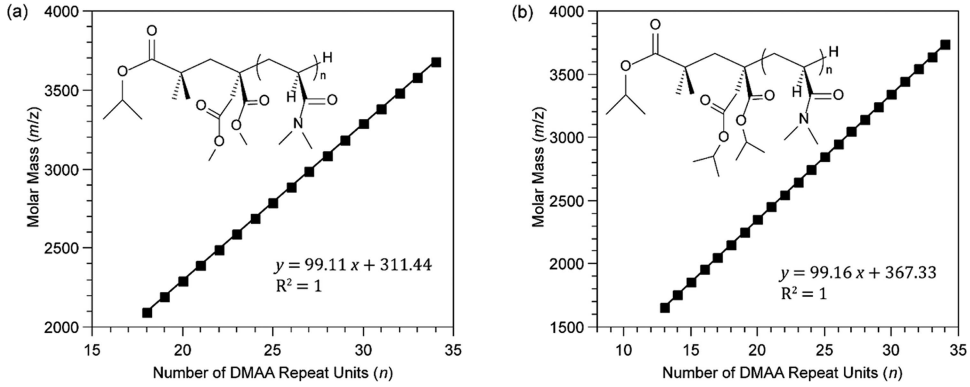


**Figure 7.** Plots of $m/z$ values vs the number of DMAA repeat units ($n$) from the MALDI-TOF spectra in Figure 6 left (a) and Figure 6 right (b).

polymer terminus derived from the original dimethyl or diisopropyl itaconate in **2a,b**, respectively. Moreover, low-molecular-weight PDMAA samples prepared by **2a,b** were analyzed by MALDI-TOF mass spectrometry (Figure 6). The plot of $m/z$ values of the spectrum peaks vs the number of DMAA repeat units gave a straight line (Figure 7), with a slope corresponding to the mass of the monomer and the intercept to the sum of the masses of $Na^+$ (from the added NaI) and the expected end group, $C_{14}H_{24}O_6$ and $C_{18}H_{32}O_6$, which is equal to the sum of $[OC(O^iPr){=}CMe_2]$ plus DMIA or D$^i$PrIA, respectively. Identical results were obtained with low-molecular-weight samples of PDMAA obtained by Zr-itaconate chelates **15a,b**, also confirming the presence of the dialkyl itaconates as part of the chain end (Figures S43−S46 in the Supporting Information). These results led to the conclusion that the polymerization of DMAA initiated by the eight-membered-ring chelates **2a,b** and **15a,b** followed the same initiation/propagation mechanism established for cationic *ansa*-zirconocene ester enolate complex $\mathbf{1}^+$ (Scheme 8).[22,23]

## CONCLUSIONS

In summary, we have investigated extensively the reactivity of neutral and cationic complexes of both bridged *ansa*-zirconocenes and unbridged zirconocenes toward biorenewal itaconic esters (itaconates) and anhydride. In this study, bridged *ansa*-zirconocene complexes are represented by $C_2$-ligated, *rac*-(EBI)Zr-based *ansa*-zirconcene mono ester enolate complex **1** and its corresponding cationic *ansa*-zirconcenium ester enolate complex $\mathbf{1}^+$, while unbridged zirconocenes are exemplified by the newly synthesized Cp*($^n$PrCp)Zr-based mono ester enolate **13** and its corresponding cationic ester enolate complex $\mathbf{13}^+$. The results of this investigation revealed similar monomer insertion and polymerization chemistry between these two classes of metallocene complexes, but some noteworthy differences as well.

*ansa*-Zirconcenium ester enolate $\mathbf{1}^+$ reacts with dialkyl itaconates such as DMIA and D$^i$PrIA to form cleanly single monomer addition products, eight-membered-ring metallacycles **2** with chelation through dative coordination of the ester group derived from the initiating ester enolate ligand to Zr. Interestingly, metallacycles **2**, as the kinetic products of this nucleophilic addition reaction, undergo slow ligand exchange between the coordinated (chelated) ester group with the noncoordinated $\beta$-alkyl ester group of the itaconates at room temperature to form thermodynamically favored seven-membered-ring chelates **4**, via the proposed five-coordinated transition state structure **3**. While cationic $\mathbf{1}^+$ reacts with IA to afford an intractable product mixture, neutral zirconocene **1** reacts cleanly with IA to afford the single IA addition product **5**. Behaving similarly, unbridged zirconocenium ester enolate $\mathbf{13}^+$ reacts with itaconates to afford the corresponding eight-membered-ring metallacycles **15**, and neutral ester enolate **13** reacts with IA to give single IA addition product **17**. However, unlike labile eight-membered chelates **2** derived from *ansa*-zirconocenium **1**, eight-membered chelates **15** derived from sterically more crowded unbridged zirconocenium **13** are stable at room temperature and do not undergo the ligand exchange to form hypothesized seven-membered ring chelates **16**.

The above cationic complexes, either before the stoichiometric reaction with itaconates or after, exhibit no reactivity toward further additions of itaconates and therefore no chain propagation and growth. On the basis of the hypothesis that the origin of this lack of polymerization activity arises from the inability of the incoming monomer to ring open the first monomer addition product, the eight-membered-ring chelate, more basic monomers such as DMAA were employed to test this hypothesis. Indeed, eight-membered metallacycles **2** (from the bridged zirconocene) and **15** (from the unbridged zirconocene), but not seven-membered **4**, effectively polymerize DMAA in a controlled manner, producing either highly isotactic PDMAA with $mm$ > 99% by **2** or PDMAA with narrow molecular weight distributions with $Đ$ = 1.14−1.19 by **15**.

## ASSOCIATED CONTENT

### Supporting Information

The Supporting Information is available free of charge on the ACS Publications website at DOI: 10.1021/acs.organomet.7b00358.

Full experimental details and additional figures (PDF)

### Accession Codes

CCDC 1548705 contains the supplementary crystallographic data for this paper. These data can be obtained free of charge via www.ccdc.cam.ac.uk/data_request/cif, or by emailing data_request@ccdc.cam.ac.uk, or by contacting The Cambridge Crystallographic Data Centre, 12 Union Road, Cambridge CB2 1EZ, UK; fax: +44 1223 336033.

## AUTHOR INFORMATION

### Corresponding Author

*E-mail for E.Y.-X.C.: eugene.chen@colostate.edu.

### ORCID

Eugene Y.-X. Chen: 0000-0001-7512-3484



DOI: 10.1021/acs.organomet.7b00358
*Organometallics* 2017, 36, 2922−2933

### Notes

The authors declare no competing financial interest.

## ■ ACKNOWLEDGMENTS

This work was supported by the U.S. National Science Foundation (NSF-1300267 and NSF-1664915). We thank Dr. Brian Newell for help with solving the crystal structure of $9^+$ and Boulder Scientific Co. for the research gifts of $B(C_6F_5)_3$ and Cp*($^n$PrCp)$ZrCl_2$.

## ■ REFERENCES

(1) Llevot, A.; Dannecker, P.-K.; von Czapiewski, M.; Over, L. C.; Söyler, Z.; Meier, M. A. R. *Chem. - Eur. J.* **2016**, *22*, 11510−11521.
(2) Yao, K.; Tang, C. *Macromolecules* **2013**, *46*, 1689−1712.
(3) Hajian, H.; Wan Yusoff, W. M. *Curr. Res. J. Biol. Sci.* **2015**, *7*, 37−42.
(4) Klement, T.; Büchs, J. *Bioresour. Technol.* **2013**, *135*, 422−431.
(5) Willke, T.; Vorlop, K. D. *Appl. Microbiol. Biotechnol.* **2001**, *56*, 289−295.
(6) Bozell, J. J.; Petersen, G. R. *Green Chem.* **2010**, *12*, 539−554.
(7) Geilen, F. M. A.; Engendahl, B.; Harwardt, A.; Marquardt, W.; Klankermayer, J.; Leitner, W. *Angew. Chem., Int. Ed.* **2010**, *49*, 5510−5514.
(8) Medway, A. M.; Sperry, J. *Green Chem.* **2014**, *16*, 2084−2101.
(9) Yang, J.-Z.; Otsu, T. *Polym. Bull.* **1991**, *25*, 145−152.
(10) Otsu, T.; Yamagishi, K.; Yoshioka, M. *Macromolecules* **1992**, *25*, 2713−2716.
(11) Otsu, T.; Watanabe, H. *Eur. Polym. J.* **1993**, *29*, 167−174.
(12) Otsu, T.; Yamagishi, K.; Matsumoto, A.; Yoshioka, M.; Watanabe, H. *Macromolecules* **1993**, *26*, 3026−3029.
(13) Fernández-García, M.; Fernández-Sanz, M.; de la Fuente, J. L.; Madruga, E. L. *Macromol. Chem. Phys.* **2001**, *202*, 1213−1218.
(14) Szablan, Z.; Toy, A. A.; Terrenoire, A.; Davis, T. P.; Stenzel, M. H.; Müller, A. H. E.; Barner-Kowollik, C. *J. Polym. Sci., Part A: Polym. Chem.* **2006**, *44*, 3692−3710.
(15) Robert, T.; Friebel, S. *Green Chem.* **2016**, *18*, 2922−2934.
(16) Vilela, C.; Sousa, A. F.; Fonseca, A. C.; Serra, A. C.; Coelho, J. F. J.; Freire, C. S. R.; Silvestre, A. J. D. *Polym. Chem.* **2014**, *5*, 3119−3141.
(17) Chen, E. Y.-X. *Chem. Rev.* **2009**, *109*, 5157−5214.
(18) Bolig, A. D.; Chen, E. Y.-X. *J. Am. Chem. Soc.* **2004**, *126*, 4897−4906.
(19) Rodriguez-Delgado, A.; Chen, E. Y.-X. *Macromolecules* **2005**, *38*, 2587−2594.
(20) Zhang, Y.; Ning, Y.; Caporaso, L.; Cavallo, L.; Chen, E. Y.-X. *J. Am. Chem. Soc.* **2010**, *132*, 2695−2709.
(21) Chen, X.; Caporaso, L.; Cavallo, L.; Chen, E. Y.-X. *J. Am. Chem. Soc.* **2012**, *134*, 7278−7281.
(22) Mariott, W. R.; Chen, E. Y.-X. *Macromolecules* **2004**, *37*, 4741−4743.
(23) Mariott, W. R.; Chen, E. Y.-X. *Macromolecules* **2005**, *38*, 6822−6832.
(24) Vidal, F.; Falivene, L.; Caporaso, L.; Cavallo, L.; Chen, E. Y.-X. *J. Am. Chem. Soc.* **2016**, *138*, 9533−9547.
(25) Vidal, F.; Gowda, R. R.; Chen, E. Y.-X. *J. Am. Chem. Soc.* **2015**, *137*, 9469−9480.
(26) Vidal, F.; Chen, E. Y.-X. *Synlett* **2017**, *28*, 1028−1039.
(27) Miyake, G.; Caporaso, L.; Cavallo, L.; Chen, E. Y.-X. *Macromolecules* **2009**, *42*, 1462−1471.
(28) Miyake, G. M.; Chen, E. Y.-X. *Macromolecules* **2008**, *41*, 3405−3416.
(29) Ning, Y.; Chen, E. Y.-X. *Macromolecules* **2006**, *39*, 7204−7215.
(30) Ning, Y.; Chen, E. Y.-X. *J. Am. Chem. Soc.* **2008**, *130*, 2463−2465.
(31) Hu, Y.; Miyake, G. M.; Wang, B.; Cui, D.; Chen, E. Y.-X. *Chem. - Eur. J.* **2012**, *18*, 3345−3354.
(32) Miyake, G. M.; Newton, S. E.; Mariott, W. R.; Chen, E. Y.-X. *Dalton Trans.* **2010**, *39*, 6710−6718.
(33) Rodriguez-Delgado, A.; Mariott, W. R.; Chen, E. Y.-X. *J. Organomet. Chem.* **2006**, *691*, 3490−3497.
(34) Collins, S.; Ward, D. G.; Suddaby, K. H. *Macromolecules* **1994**, *27*, 7222−7224.
(35) Li, Y.; Ward, D. G.; Reddy, S. S.; Collins, S. *Macromolecules* **1997**, *30*, 1875−1883.
(36) Collins, S.; Ward, D. G. *J. Am. Chem. Soc.* **1992**, *114*, 5460−5462.
(37) Mariott, W. R.; Rodriguez-Delgado, A.; Chen, E. Y.-X. *Macromolecules* **2006**, *39*, 1318−1327.
(38) Ning, Y.; Caporaso, L.; Correa, A.; Gustafson, L. O.; Cavallo, L.; Chen, E. Y.-X. *Macromolecules* **2008**, *41*, 6910−6919.
(39) Zhang, Y.; Caporaso, L.; Cavallo, L.; Chen, E. Y.-X. *J. Am. Chem. Soc.* **2011**, *133*, 1572−1588.
(40) He, J.; Zhang, Y.; Chen, E. Y.-X. *Macromol. Symp.* **2015**, *349*, 104−114.



DOI: 10.1021/acs.organomet.7b00358
*Organometallics* 2017, 36, 2922−2933